Vol. 15, pp. 214–228 (2018)
doi: 10.2142/biophysico.15.0_214

Biophysics and Physicobiology

https://www.jstage.jst.go.jp/browse/biophysico/

Regular Article

Verification of the effect of the axon fluid as a highly dielectric medium in the high-speed conduction of action potentials using a novel axon equivalent circuit

Takayoshi Tsubo and Makoto Kurokawa

Department of Biological Sciences, Tokyo Metropolitan University, Hachioji, Tokyo 192-0397, Japan

Received March 9, 2018; accepted September 14, 2018

Both sensory neurons and motor neurons transfer signals rapidly through long pathways. Such signals propagate as action potentials through neurons. In myelinated neurons, high conduction velocities of 120 m/s have been reported, even for axons of just 20 μm in diameter. Such a high conduction velocity is enabled by the characteristic morphology of a myelinated axon: repeated regions encased by long uniform myelin sheaths alternating with extremely short exposed regions of the axon called nodes of Ranvier, which generate extremely sharp action potentials. Although the need for the action potential to cross many nodes increases the relay time, it is still able to propagate rapidly. This phenomenon motivated us to derive a new mechanism of the action potential propagation. First, the dielectric effect of the axonal fluid was considered, and it was investigated whether the combination of the characteristic axonal morphology and the dielectric constant of the axonal fluid contributes significantly to the realization of high conduction velocities even with the inclusion of a large loss in the relay time. To this end, we propose a new axon equivalent circuit that incorporates the effect of the dielectric characteristics of the axonal fluid. It was confirmed that a realistically high conduction velocity could be calculated using the proposed circuit and that the dielectric constant calculated using the proposed circuit was in agreement with that of an ionic fluid similar to axonal fluid. Moreover, the contribution of the combination of the axonal morphology and axonal fluid to the conduction velocity was confirmed.

Key words: myelinated sheath, node of Ranvier, distributed-element circuit, capacitance, displacement current

Corresponding author: Takayoshi Tsubo, Department of Biological Sciences, Tokyo Metropolitan University, 1-1 Minamiosawa Hachioji, Tokyo 192-0397, Japan.
e-mail: Tsubo-takayoshi@ed.tmu.ac.jp

1. Introduction

The ability of animals to capture prey—or to flee predators rapidly—requires the high-speed transmission of both sensory signals from sensory organs to the brain and motor control signals from the brain to the muscles. Such signals propagate as action potentials along neurons [1,2]. High conduction velocities of up to 120 m/s have been reported for myelinated neurons, even those with axons just 20 μm in diameter [3–6]. This high velocity is enabled by the characteristic morphology of the myelinated axon, shown in Figure 1a; this morphology consists of regions enveloped by long and uniform myelin sheaths alternating with extremely short gaps called nodes of Ranvier at which extremely sharp action potentials are generated [1]. As a consequence of this morphology, action potentials are relayed from node to node

◀ *Significance* ▶

To verify the mechanism of the high conduction velocity of an action potential, we proposed a new axon equivalent circuit that incorporates the effect of the dielectric characteristics of axon fluid. It was confirmed that a high-speed conduction velocity could be calculated with the proposed equivalent circuit and that the dielectric constant of an ionic fluid similar to axon fluid was similar to that calculated using the proposed equivalent circuit. Moreover, the contribution of the combination of the axon morphology and the axon fluid to the conduction velocity was confirmed.

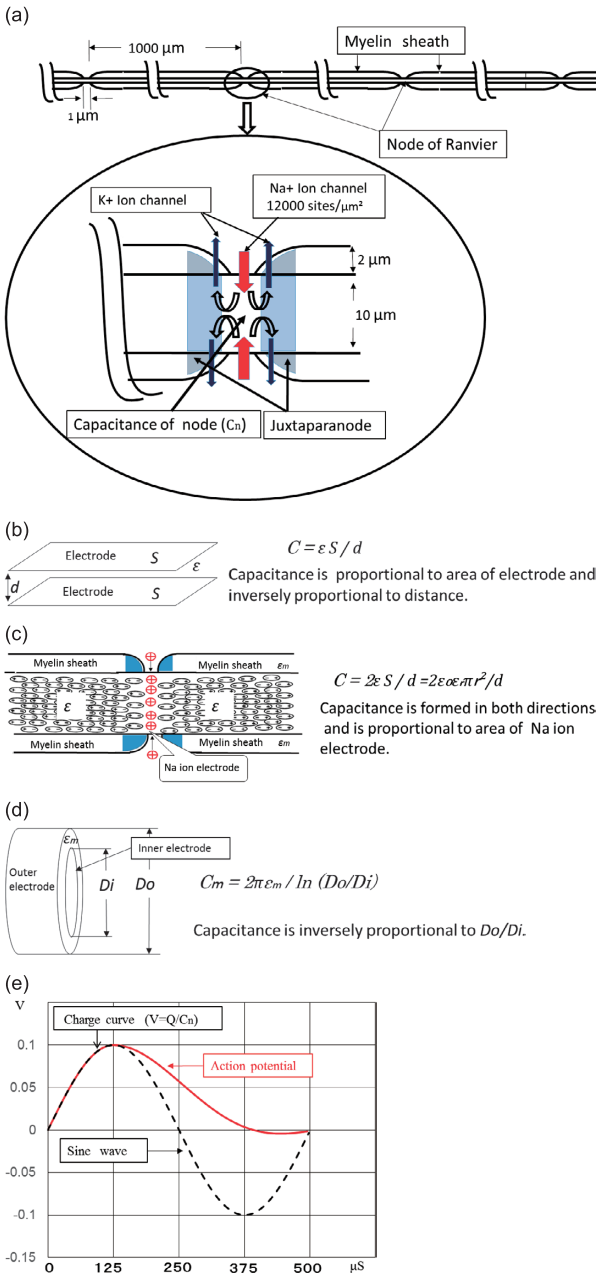

Figure 1 (a) Myelin sheath and node of Ranvier; (top) The length of the myelin sheath is about 1000 times longer than that of a node of Ranvier; (bottom) Positively charged Na^+ ions flow through Na ion channels into the disc-shaped area of capacitance C_n of the node of Ranvier; subsequently, an equivalent positive charge carried by K^+ ions is expelled through K^+ ion channels. Two local ion current loops are formed by Na^+ ion channels in the node and K^+ ion channels on both sides of the node. (b) Capacitance by parallel plate electrodes. This equation is normally used to calculate the capacitance of a condenser. (c) Capacitance of a Na ion electrode. This equation was defined to calculate the axonal longitudinal capacitance in this study. (d) Capacitance by Do/Di. This equation is used to calculate the capacitance of a cylinder-like myelin sheath. (e) Action potential and sine wave. An influx of positively charged Na^+ ions into the disc-shaped area of capacitance C_n of the node of Ranvier results in an increase of positive charge Q, and that makes action potential high as shown by the equation (V = Q/Cn). Between the initial point and the peak value, the action potential waveform (red curve) resembles a sine wave (black dashed curve) of 2 kHz.

via mechanism called saltatory conduction [7–9], and this relay occurs extremely many times in long motor or sensory neurons because action potential is quickly attenuated in a short length and each relay operation takes time. Because of this, the conduction velocity of the action potential is influenced by the time loss of relay of action potential rather than the propagation speed of the action potential. Therefore, the actual propagation speed of an action potential itself (hereafter called the raw velocity) may be more than 10 times the conduction velocity which includes the large relay time loss. In our study, a significantly low raw velocity of 82 m/s which is less than 1/10 times the raw required velocity which is 1200 m/s (120 m/s × 10) ,was calculated in an axon of 20 µm in diameter using the distributed-element circuit approach for a conventional general axon equivalent circuit [10–13]. This large difference in raw velocity indicates that there is another carrier of action potentials apart from conventional charged particles which propagates through the axonal resistance. That new carrier is the propagation of electric field produced by polarization of dielectric medium of axon fluid generated by action potential. Therefore, in this study, we considered that propagation of the electric field by polarization of the axon fluid activates the voltage-gated Na channels [14] of distant nodes. This indicates that high-speed conduction may be achieved by a combination of the characteristic axonal morphology and the dielectric properties of the axon fluid, even if a large relay time is involved.

1.1 Three factors determining conduction velocity and the wave equation of the action potential

The conduction velocity v of an action potential is determined mainly by the numerous relays time as the action potential relay from node to node, as described above. Therefore, v is determined by three elements: the relay interval x, the travel time t to the relay point x at the raw velocity Vr, and the relay time τ which is the rise time of the action potential at point x. The equation $v = x/(t + \tau)$ was devised to express v in terms of these three elements. The first term t in the denominator corresponds to the travel time x/Vr. And to determine τ of the second term in the denominator, the attenuation of the action potential by a factor $1/e^{\alpha x}$ as a result of traveling the distance x must be considered. This means that the wave equation of the action potential must be defined such that it gives an attenuation constant α and a phase constant β which determines the raw velocity Vr [15].

1.2 Role of the dielectric characteristics of the axon fluid

Because axon fluid is a solution in which ions are dissolved in water, which has a high dielectric constant with orientation polarization [16], it can be considered as a strong dielectric medium. The dielectric constant is proportional to the relative permittivity ε_r. The relative permittivity ε_r is the ratio of dielectric constant ε of the medium to the permittivity ε_0 of a vacuum. It is an index that indicates the ease with which a medium is polarized and makes an electric field.

The dielectric constant and permittivity express the same characteristic. That is, if an electric charge σ exists in a dielectric medium, one of Maxwell's equations ($\sigma = \varepsilon\nabla\cdot\mathbf{E} = \nabla\cdot\mathbf{D}$) states that an electric flux density **D** proportional to the dielectric constant ε of the dielectric medium forms and broadens around the electric charge σ [15]. **E** and **D** are the vector representations of the electric field and the electric flux density; however, in this paper, **D** is hereafter referred to simply as the electric field. A strong electric field **D** proportional to the axonal dielectric constant ε occurs when there is a large quantity of Na^+ ions in a node of Ranvier, as shown in Figure 1a. Furthermore, one of Maxwell's equations $Id = d\mathbf{D}/dt$ shows that the displacement current Id is generated in proportion to the rate of change of the electric field **D** [15]. The displacement current Id increases the propagation velocity of the electric field. If the electric field **D** reaches the threshold of a voltage-gated Na channel of a distant node of Ranvier, and triggers to generate an action potential, it indicates that electric field **D** and displacement current Id play the role of propagating action potential as a new carrier.

1.3 Dielectric characteristics and longitudinal capacitance of axon fluid

To model the axon fluid in an equivalent circuit of the axon, it is necessary to quantitatively define the role of the dielectric characteristics of the axon fluid as capacitance. And a new capacitance that plays the role of a carrier by the dielectric medium must be attached in parallel with the axonal resistance of the pathway for charged particles. Therefore, the longitudinal capacitance was defined as follows for inclusion in the newly proposed equivalent circuit of the axon. The essence of the capacitance is a polarization of the dielectric medium. Generally, a capacitor consists of two electrodes, as shown in Figure 1b. By applying a voltage across the two electrodes, the dielectric medium contained between them becomes polarized. Therefore, one electrode can be used if there exists an alternative method of polarizing the dielectric medium. In an axon, the existence of a net positive electric charge produced by a large number of Na^+ ions flowing into the axon to produce an action potential at a node of Ranvier functions as an electrode and causes the dielectric medium of the axon fluid to become polarized. An electric field proportional to the dielectric constant of the axon fluid induced by the polarization is thus propagated in both directions longitudinally along the axon. The electric field generated by each action potential spreads out equally in both longitudinal directions if a new action potential is generated at the adjacent node of Ranvier. Therefore, as shown in Figure 1c the longitudinal capacitance C_1 is considered to be given by $C_1 = 2\varepsilon S/d$, where the factor of 2 indicates the contribution of the two directions, ε is the dielectric constant, S is the area of the node of Ranvier where the positive electric charge from the Na^+ ions is located, and d is the distance from the electrode of the node.

1.4 Relation between axonal morphology and action potential speed

As stated previously, myelinated neurons have a characteristic morphology consisting of repeated regions encased by long and uniform myelin sheaths [4,17] alternating with extremely short gaps called nodes of Ranvier, which generate extremely sharp action potentials [18]. The membrane capacitance C_m of the myelin sheath greatly depends on the thickness of the sheath membrane [19], as shown in Figure 1d. The membrane of the myelin sheath is composed of several hundred thin layers of myelin. Increasing the sheath thickness effectively increases the ratio of the outer diameter to the inner diameter of the axon, thereby decreasing the membrane capacitance and increasing the membrane resistance [20]. In other words, the myelin sheath acts as a long uniform cylinder of high impedance. Nodes of Ranvier are very short, with lengths of approximately 1/1000 of the length of a myelin sheath. This causes the capacitance C_n of the nodes of Ranvier to be very small, as shown in Figure 1a. These nodes also contain a very high density of Na channels embedded in the membrane, allowing a large quantity of Na^+ ions to flow into the axon in a short time when an action potential is produced. This generates a large net positive electric charge Q as a result of the sudden influx of Na^+ ions in this region of small capacitance C_n. The structure of the node of Ranvier is suitable for generating a large voltage and a steep displacement current by a large and a steep action potential [21]. Therefore, the structure of the node of Ranvier produces an increase in leakage electric current I_m which is the displacement current I_m ($= C_m dV/dt$) of the membrane capacitance C_m. Therefore, it may be said that the structure of the myelin sheath which is made to reduce the leakage current, and the structure of the node of Ranvier which is made to increase leakage current by a large displacement current, are mismatched. However, the effect of the axon fluid acting as a new carrier is increased by the structure of the node of Ranvier generating a rapid change in the action potential. In this study, using the variable number indicating the rate of change of the action potential, the degree of the mismatch of the structure mentioned above and the validity of handling the axon fluid as a new carrier of the electric field were investigated.

2. Methods

This chapter describes the methods used in this study to demonstrate that the high conduction velocity of the action potential is achieved by a combination of the axon fluid acting as a carrier of the electric field and the characteristic morphology of the axon.

2.1 Calculation environment, calculation software, and unit system

In this study, a partial differential equation with respect to time and position was considered; however, the final equa-

Table 1 Data about the axon

Variable	Location	Data assembled by Hodgkin [a]	Myelinated axon [b]		
			20 μm	13 μm	6 μm
	Diameter (outer) of axon	14 μm	28 μm	18.2 μm	8.4 μm
	Diameter (inner) of axon	10 μm	20 μm	13 μm	6 μm
	Thickness of myelin	2 μm	4 μm	2.6 μm	1.2 μm
R1	Resistance per unit length of axis cylinder	14,000 MΩ/m	3,500 MΩ/m	8,284 MΩ/m	38,888 MΩ/m
R2	Resistance × unit length of myelin sheath	0.25–0.4 MΩ m	0.32 MΩ m	0.32 MΩ m	0.32 MΩ m
C1	Capacity per unit length of axis cylinder	Not defined	7.409×10^{-14} F m	3.130×10^{-14} F m	6.668×10^{-15} F m
C2	Capacity per unit length of myelin sheath	1,000–1,600 pF/m	1300 pF/m	1300 pF/m	1300 pF/m
	Relative permittivity of myelin sheath	5–10	5–10	5–10	5–10
	Length of myelin sheath [c]		2 mm	1.3 mm	0.6 mm
	Length of the node of Ranvier		2 μm	1.3 μm	0.6 μm
Cn	Capacity of the node of Ranvier	0.6–1.5 pF			

[a] This column includes data of the frog myelinated nerve originally obtained by Huxley and Stampfli (1949) and by Tasaki (1955) and compiled by Hodgkin in 1964 [19].
[b] These data were obtained by applying the conversion formulas of section 2.4 to axons of various diameters.
[c] These data were obtained from reference document [4].

tion derived from this is a simple expression using the circuit constants R_1, R_2, C_1, and C_2 and the angular velocity ω. Therefore, the calculation environment is a normal PC, and the calculation and drawing software is the standard office application Microsoft Excel (Microsoft Corporation). The circuit constants and solutions were assessed in the MKS unit system; that is, the unit length, weight, time, and speed were considered to be 1 m, 1 kg, 1 s, and 1 m/s, respectively.

2.2 Longitudinal capacitance applied to the axon equivalent circuit

As mentioned in section 1.3, the longitudinal capacitance C_1 is defined as

$$C_1 = 2\varepsilon S/d = 2\varepsilon_0\varepsilon_r\pi r^2/d \quad (1)$$

where the factor of 2 corresponds to the contribution from the two directions longitudinally along the axon, ε is the dielectric constant of the axon fluid, ε_0 ($= 8.854 \times 10^{-12}$) is the permittivity of a vacuum, and the relative permittivity ε_r is the ratio of the dielectric constant ε of the axon fluid to permittivity of a vacuum ε_0. In addition, S is the axonal cross section; r is the axonal radius, where the radii of the axon and the node of Ranvier are equal [22,23]; and d is the distance from the electrode. The capacitance C_1 is merely inversely proportional to the distance d. Because the relative permittivity ε_r of the axon fluid is much larger than that (5–10) of the axonal membrane (Table 1), the electric field propagates mostly in both directions along the longitudinal axis of the axon with negligible diffusion towards the axonal membrane. This is why the longitudinal capacitance C_1 is inversely proportional to the distance d linearly, not the square of the distance d.

2.3 Membrane capacitance of the myelin sheath

The membrane capacitance C_2 of the cylindrical myelin sheath was calculated as

$$C_2 = C_m = 2\pi\varepsilon_m / ln\,(D_o/D_i) \quad (2)$$

where ε_m is the dielectric constant of membrane of the myelin sheath, ln expresses a natural logarithm and D_o and D_i are respectively the outer and inner diameter of the axon [15], as shown in Figure 1d.

2.4 Relationship between the circuit constants and axon diameter

Longitudinal axonal resistance R_1 is inversely proportional to the square of the diameter, and capacitance C_1 is proportional to the square of the diameter of the axon. However, membrane resistance R_2 and membrane capacitance C_2 of the myelin sheath are independent of the diameter of the axon. Berthold *et al.*'s study [24] states that thickness of the myelin sheath is proportional to diameter of axon. In their study, increasing the diameter makes the membrane thick, which increases the membrane resistance and results in a wide area of inner wall of the axon that decreases the membrane resistance. Therefore, the effect of the change in diameter of the axon is cancelled. As for the membrane capacitance C_2, the above reference [24] states that the ratio of the outer and inner diameter remains constant, even if the diameter changes. Therefore, the membrane capacitance C_2 does not change, because the capacitance of a cylinder such as a myelin sheath is calculated using the dielectric constant and the ratio of the outer and inner diameters. Based on these relationships, the circuit constants were set as given in Table 1.

2.5 Conventional axon equivalent circuit and axon equivalent circuit with applied dielectrics

In the conventional representative axon equivalent circuit, circuits representing the node of Ranvier and the myelin sheath region alternate sequentially, as shown in Figure 2a and b [10,12]. In a myelinated nerve, the ratio of the length of the node of Ranvier to that of the myelin sheath is approximately 1/1000 [17,18]. For this case, the propagation speed and attenuation coefficient were calculated for the myelinated region, and the influence of these factors on the unmyelinated nodes of Ranvier were investigated using the calculation results. Therefore, the myelin sheath region was first considered in the development of the axon equivalent circuit. Figure 2c and d shows a representative conventional axon equivalent circuit and the newly proposed axon equivalent circuit including the dielectric constant of the axon fluid, respectively. The only difference between the two equivalent circuits is the addition of the longitudinal capacitance C_1 considered as a new signal transmission carrier between A and B in the proposed circuit (Fig. 2d). In addition, in both equivalent circuits, an action potential generated between A and C propagates along the axon from A to B. However, if a signal propagates from B to C, this indicates that the action potential has leaked out from the axon to the extracellular space through the membrane of the myelin sheath. Therefore, if the electric potential at B in the node of Ranvier reaches the threshold of the voltage-gated Na channels in the node of Ranvier, these channels activate and generate an action potential; this behavior of the node of Ranvier is not represented in the depicted axon equivalent circuit.

2.6 Influence of the axon equivalent circuit on input signals

Both axon equivalent circuits are characterized by the form of a ladder-type circuit with resistive and capacitive components. An input signal is able to pass through such a circuit without influence by reflection. Therefore, regardless of the overall shape of the action potential signal input into these axon equivalent circuits, the input signal can propagate without colliding with a reflection from the circuit. An action potential will thus activate a voltage-gated Na channel when the rising phase of the action potential reaches the threshold of the voltage-gated Na channel [14]. Therefore, the propagation of the rising phase from the start to peak of the action potential (1/4 period of sine wave in Fig. 1e) is the most important aspect and the waveform after the peak is inconsequential for the propagation of action potential.

2.7 Amplitude and rise time of action potential

When the electric potential of a propagating action potential exceeds the threshold of the voltage-gated Na channels at a node of Ranvier, an action potential begins to be generated at that node. These nodes are very narrow, with a capacitance of 0.6–1.5 pF (Table 1), a width of 2 µm, and a

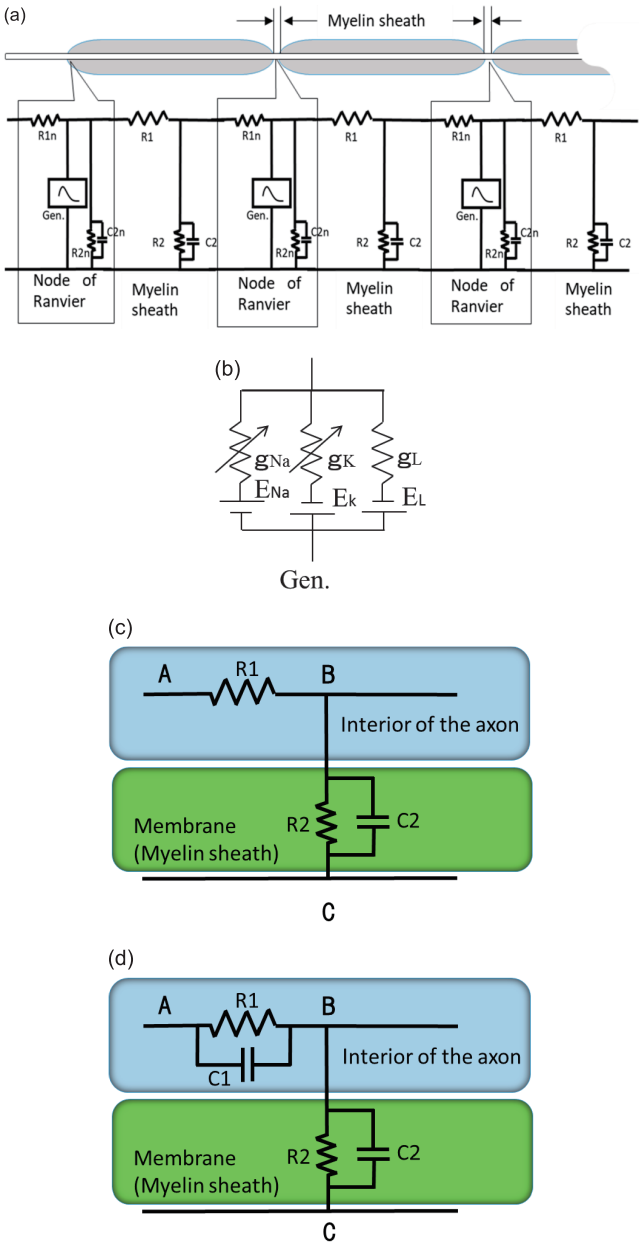

Figure 2 (a) Sample conventional axon equivalent circuit; When *Gen*. provides high impedance, an axonal longitudinal resistor *R1*, membrane resistor *R2*, and membrane capacitance *C2* are present at the myelin sheath region, and an axonal longitudinal resistor *R1n*, membrane resistor *R2n*, and membrane capacitance *C2n* are present at the node of Ranvier region. Those resistors and capacitances constitute a ladder circuit that does not reflect back a signal regardless of the terminal condition. (b) Action potential generator; Gen. is the action potential generator. gL and EL produce voltage during the resting situation. gNa and ENa insert Na^+ ions into the axon, and gK and EK allow flow of the same quantity of K^+ ions as Na^+ ions that flow out of the axon. (c) Conventional axon equivalent circuit; (d) Axon equivalent circuit with applied dielectrics. The difference between the conventional axon equivalent circuit in Figure 2c and the axon equivalent circuit with applied dielectrics in Figure 2d is the existence of axonal longitudinal capacitance *C1*.

diameter of 10 μm. However, the density of voltage-gated Na channels is very high at 12,000 sites/μm² [25], and a total of 753,600 voltage-gated Na channels are present in the axonal membrane of the node. Na^+ ions with an electric charge of 1.6×10^{-19} Coulombs per particle rapidly flow into the axon fluid through these voltage-gated Na channels, and a net positive charge Q of 1.2048×10^{-13} Coulombs is charged to the capacitance of the node ($C_n = 0.6$–1.5 pF). Therefore, the peak voltage V of the action potential is approximately 80–200 mV [26–28], as given by the equation $V = Q/C_n$. It is thought that the rate of voltage increase of the action potential is very high because a large quantity of Na^+ ions suddenly enters the intracellular space at the node of Ranvier via the rapid activation of all of the voltage-gated Na channels at the node. In this study, the amplitude of the action potential was set to 100 mV as a general representative quantity, as shown in Figure 1e. The rise time was set to 125 μs by modeling the rising phase of the action potential as the first quarter period of a sine wave with a frequency of 2 kHz; this rise time was selected based on previously reported values [29].

2.8 Definition of the waveform of the action potential

The waveform of the rising phase of the action potential is similar to the first quarter period of a sine wave, which also resembles a charge curve (Fig. 1e). Moreover, because the waveform after the peak does not affect the propagation of action potential as mentioned in the section 2.6, action potentials were modeled as an entire period of a sine wave. Because the circuits contain capacitors, the complex representation that is generally used to express the voltage in an electric circuit was employed here so that calculations including phase shifts are possible [15]. Thus, the action potential waveform considered here is given by

$$V e^{j\omega t} = W \sin(\omega t)\, e^{j\omega t} = W \sin(\omega t)\, (\cos(\omega t) + j \sin(\omega t)) \tag{3}$$

where j is the imaginary part, ω is the angular velocity, and W is the max amplitude of the sine wave representing the action potential.

2.9 Equations for the axon equivalent circuits

The equivalent circuit for the myelin sheath region of the axon (Fig. 2c and d) consists of uniform impedance in the AB and BC segments, whose length ranges from infinitesimal to long. Therefore, the raw velocity Vr and attenuation constant α can be accurately calculated using the distributed-element circuit approach. The main purpose of this study was to confirm the effect of the longitudinal capacitance of the axon fluid as a newly proposed carrier of propagating action potentials. For both axon equivalent circuits, an action potential was generated at point A in the form of the voltage function $V = V_1 e^{j\omega t}$; then, the voltage drop over the infinitesimal segment AB (in the longitudinal direction) and the current flowing between points B and C (through the axonal membrane to the extracellular space) are given by the following action potential conduction equations.

In the conventional axon equivalent circuit:

$$-\mathrm{d}V/\mathrm{d}x = R_1 I = ZI \tag{4}$$

$$-\mathrm{d}I/\mathrm{d}x = V/R_2 + C_2(\mathrm{d}V/dt) = (1/R_2 + j\omega C_2)V = YV. \tag{5}$$

In the axon equivalent circuit with applied dielectrics:

$$-\mathrm{d}V/\mathrm{d}x = I/(1/R_1 + j\omega C_1) = ZI \tag{6}$$

$$-\mathrm{d}I/\mathrm{d}x = V/R_2 + C_2(\mathrm{d}V/\mathrm{d}t) = (1/R_2 + j\omega C_2)V = YV. \tag{7}$$

For these two circuits, Equations (4) and (6) were differentiated with respect to x, and $\mathrm{d}I/\mathrm{d}x$ on the right-hand sides of the resulting equations was substituted by the left-hand side of equations (5) and (7). This yielded

$$\mathrm{d}^2V/\mathrm{d}x^2 = ZYV. \tag{8}$$

The quantity Z was defined differently for the two types of circuits but took the same general form, and the solution is given by

$$\begin{aligned} V &= V_1 e^{-\sqrt{ZY}X} + V_1 e^{\sqrt{ZY}X} = V_1 e^{-\sqrt{P+jQ}X} + V_1 e^{\sqrt{P+jQ}X} \\ &= V_1 e^{-(\alpha+j\beta)X} + V1 e^{(\alpha+j\beta)X}. \end{aligned} \tag{9}$$

Because ZY includes complex numbers, it is convenient to separate the real and imaginary parts as

$$ZY = P + jQ = (\alpha + j\beta)^2. \tag{10}$$

Because the real part is needed to reach the threshold of the voltage-gated Na channels, the imaginary part was ignored. Additionally, V_1 was substituted by $W \sin(\omega t)\, e^{j\omega t}$, yielding

$$V = W \sin(\omega t) e^{-\alpha x} \cos(\omega t - \beta x) + W \sin(\omega t) e^{\alpha x} \cos(\omega t + \beta x). \tag{11}$$

Equation (11) represents the wave equation of the action potential. The first term of Equation (11) describes a cosine wave with an amplitude of $W \sin(\omega t)$ propagating in the positive x-direction with raw velocity Vr ($= \mathrm{d}x/\mathrm{d}t = \omega/\beta$) and attenuating by a factor of $e^{-\alpha x}$ ($= 1/e^{\alpha x}$) after traversing a distance of x. The second term describes a wave propagating with the same velocity and attenuation in the negative x-direction. Thus, as illustrated in Figure 3, Equation (11) indicates that an action potential generated at a node of Ranvier ($x = 0$) propagates in both directions longitudinally along the axon with attenuation according to the attenuation constant α. Correspondence was then established between the circuit constants and the real and imaginary parts P and Q of ZY in Equation (10), as shown below.

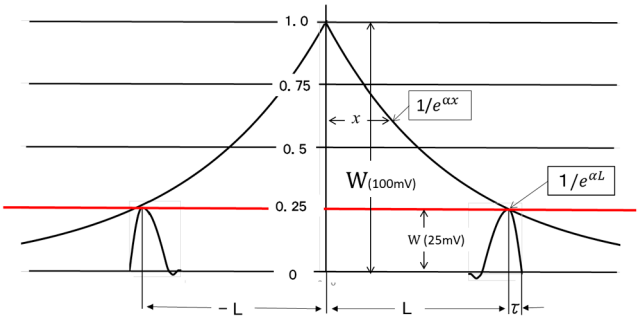

Figure 3 Propagation of the action potential. An action potential generated at a node of Ranvier propagates to the left and to the right with raw velocity Vr while decaying by a factor $1/e^{\alpha x}$ after traveling distance x. Nodes of Ranvier lying beyond the maximum reachable distance L do not fire, but nodes of Ranvier lying within that distance do fire. Needless to say, nodes of Ranvier to the left are in a refractory period and thus cannot fire. From this figure, conduction velocity v_L can be calculated by the equation $v_L = L/(L/Vr + \tau)$, in the case of a relay interval of maximum reachable distance L.

In the conventional axon equivalent circuit, P and Q are given by

$$P = R_1/R_2 \tag{12}$$

$$Q = \omega R_1 C_2. \tag{13}$$

In the axon equivalent circuit with applied dielectrics, P and Q are given by

$$P = (1/(R_1R_2) + \omega^2(C_1C_2))/((1/R_1)^2 + (\omega C_1)^2) \tag{14}$$

$$Q = \omega(C_2/R_1 - C_1/R_2)/((1/R_1)^2 + (\omega C_1)^2). \tag{15}$$

Using Equation (10) to construct relationships between the real and imaginary parts P and Q and the attenuation and phase constants α and β yielded

$$\alpha = \sqrt{(P + \sqrt{P^2 + Q^2})/2} \tag{16}$$

$$\beta = \sqrt{(-P + \sqrt{P^2 + Q^2})/2} \tag{17}$$

The phase constant β, which determines the raw velocity Vr, and the attenuation constant α, which determines the attenuation, can be expressed simply as functions of the circuit constants R_1, R_2, C_1, and C_2 and the angular velocity ω. Therefore, these equations can be solved using a general PC with Microsoft Excel. From the attenuation constant α, the remaining fraction h of the action potential amplitude after traveling a distance x was calculated as

$$h = 1/e^{\alpha x}. \tag{18}$$

The raw velocity Vr was calculated from the angular velocity and phase constant β given by Equation (11) as

$$Vr = \mathrm{d}x/\mathrm{d}t = \omega/\beta = 2\pi f/\beta. \tag{19}$$

2.10 Maximum reachable distance

The maximum reachable distance L was defined as the distance at which the peak value of the action potential attenuated to the level of the threshold of the voltage-gated Na channels, as shown in Figure 3. Therefore, nodes of Ranvier within the maximum reachable distance L from an activated node of Ranvier can generate an action potential, but more distant nodes of Ranvier cannot. The maximum peak value of the action potential was considered to be 35 mV on the basis of the assumption that the amplitude of the action potential is $W = 100$ mV and the resting potential of the axon fluid is the conventionally accepted value of −65 mV [30,31]. Additionally, the threshold of the voltage-gated Na channel was considered to be −40 mV [14]. Thus, L is given at the distance at which the reduced amplitude w becomes 25 mV. The remaining fraction h of the action potential at the maximum reachable distance L is then given by w/W, which is equal to 1/4 for $W = 100$ mV and $w = 25$ mV, as considered here. Substituting $x = L$ and $h = 1/e^{\alpha L} = w/W$ into the equation for the remaining amplitude fraction (Equation (18)) yields

$$L = \ln(W/w)/\alpha. \tag{20}$$

2.11 Equation for conduction velocity

From the equation for the wave equation of the action potential (Equation (11)), the change in the amplitude of the action potential with propagation distance x and time t. Equation (11) indicates that the amplitude with respect to time is W and that this amplitude attenuates with increasing distance x; additionally, the wave propagates with a raw velocity of $Vr = \omega/\beta$. If the attenuated action potential exceeds the threshold w of the voltage-gated Na channels at a node of Ranvier, the node of Ranvier will fire. Thus, the conduction velocity v is given by

$$v = x/(t + \tau) = x/\{(x/Vr) + A\sin(w/W/(1/e^{\alpha x}))/\omega\}. \tag{21}$$

The second term in the denominator of this equation is the rise time τ (relay time τ) at a distance of x as shown in Figure 4a. Substituting the distance $x = L$ when the relay point is at the maximum reachable distance L yields the following result. From $1/e^{\alpha L} = w/W$, the term $A\sin(w/W/(1/e^{\alpha x}))/\omega$ becomes $A\sin((w/W)/(w/W))/\omega = \pi/2/\omega = \pi/2/2\pi f = 1/4f = \tau$; thus, the rise time is 1/4 of the period of the sine wave. In other words, the peak value of the sine wave at this point is equal to the threshold of the voltage-gated Na channel at the maximum reachable distance L, in accordance with the definition given previously. From this, the conduction velocity v_L at the maximum reachable distance is given by

$$v_L = L/(L/Vr + \tau) = L/(L/Vr + 1/4f) \tag{22}$$

Equation (22) is calculated with the maximum reachable distance L, the frequency f and the raw velocity Vr. Equation (21) is used to calculate the maximum conduction velocity v

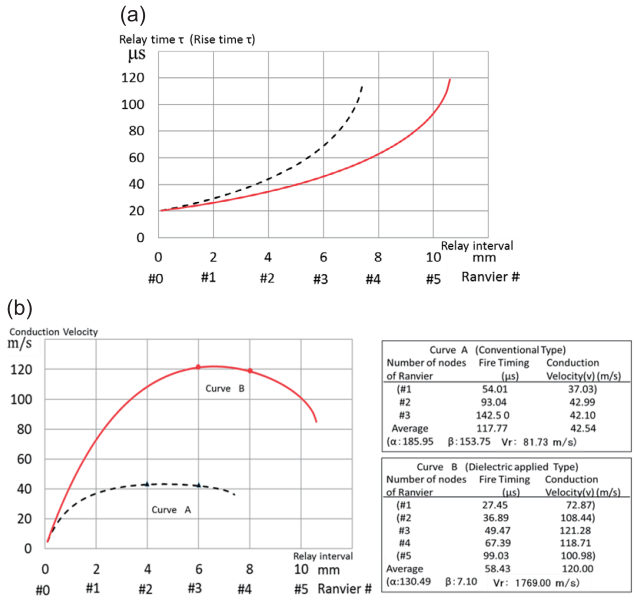

Figure 4 (a) Relay time τ (rise time τ) and relay interval x; (b) Conduction velocity v and relay interval x. Relay time τ increases exponentially near maximum reachable distance L as shown in Figure 4a. Fire timing is obtained by adding travel time t (x/Vr) and this relay time τ. And conduction velocity v is obtained by dividing distance x of the node of Ranvier (relay interval x) by fire timing ($t+\tau$). (b) shows the relation of relay interval x and conduction velocity v, in an axon of diameter 20 μm with a rise time frequency of 2 kHz. Curve A shows conduction velocity v as computed using the conventional axon equivalent circuit with the Type I values of α and Vr from Table 2. Curve B shows conduction velocity v as computed using the axon equivalent circuit with applied dielectrics with the Type II values of α and Vr from Table 2.

against the relay interval x based on a given attenuation constant α and raw velocity Vr, as shown in Figure 4b. Therefore, we must calculate using Equation (22) the attenuation constant α and raw velocity Vr against the target conduction velocity v before using Equation (21). The maximum conduction velocity is calculated using the ratio of the results of Equations (21) and (22).

2.12 Preconditions and definitions in this study

In this study, the axon fluid was newly considered as a carrier conveying the action potential, and the mechanism underlying the high conduction velocity of action potentials was elucidated based on this assumption. To this end, the following preconditions and definitions were considered in this study. However, it should be noted that these preconditions and definitions can be considered correct if it is demonstrated that (1) the dielectric constant (relative permittivity) of the axon fluid required using the dielectric applied axon equivalent circuit to achieve the conduction velocity of 120 m/s in an axon of 20 μm in diameter is equal to the actual measured dielectric constant (relative permittivity) of the axon fluid, (2) the ratio of conduction velocity v with the axon diameter is the same even if diameter of axon of the axon equivalent circuit with applied dielectrics is changed, as mentioned in the document [3,4].

a. On the basis of its dielectric properties, the axon fluid was newly considered as a carrier conveying action potentials.
b. The longitudinal capacitance was defined in accordance with the dielectric constant and cross section of the axon fluid.
c. The rising phase of the action potential was considered to correspond to the charging of the capacitor C_n by Na^+ ions, and the waveform of this charge curve was modeled as the first quarter phase of a sine wave.
d. The action potential, which is a soliton, was considered to be representable by a periodic function because there is no reflection from the circuit, a ladder-type circuit with resistive and capacitive components.
e. A collision of action potentials is a collision of each wave equation. Each wave has its own generated timing and place. (See section 4.4)

3. Results

From the equations described in the previous section, the effect of the dielectric constant of the axon fluid, newly considered here as a carrier of the action potential, was assessed, and the results are listed and shown graphically in this section. With the angular velocity as a variable, the calculation results of the conventional and proposed axon equivalent circuits are shown based on analysis in Microsoft Excel. Moreover, the relationship between the conduction velocity and the axon diameter in the proposed axon equivalent circuit with applied dielectrics was derived using axons of different diameters. The results are presented in the MKS unit system, as mentioned previously.

3.1 List of calculation results of two axon equivalent circuits

Table 2 lists the calculation results of the two axon equivalent circuits. The upper and lower halves of the table indicate the conventional axon equivalent circuit and the proposed axon equivalent circuit with applied dielectrics, respectively. The only difference between the two circuits is the inclusion of the longitudinal axonal capacitance C_1 in the proposed circuit. C_1 was set to yield a conduction velocity v of 120 m/s at 2 kHz. The column labeled f indicates the frequency of the sine wave, ranging from 1 to 4000 Hz. The column labeled ω indicates the angular velocity, which is equal to $2\pi f$, and the column labeled τ indicates the rise time to a peak of 1/4f. R_1, R_2, and C_2 are circuit constants specified in the column corresponding to an axon diameter of 20 μm in Table 1. The columns labeled P and Q indicate the real and imaginary parts of ZY. P and Q of conventional circuit are given by Equations (12) and (13), and P and Q of the proposed circuit are given by Equations (14) and (15). The columns labeled α and β indicate the attenuation and phase

Table 2 List of calculation results of two axon equivalent circuits

Type	f	ω	τ	R1	R2	C1	C2	P	Q	α	β	Vr	L	v	Nodes/L	Wave-length
Type I	1	6.28318	0.25	3.5×10^{9}	320000	0	1.3×10^{-9}	10937.5	28.588	104.58	0.14	45.970	0.01326	0.07	6.63	45.970
	5	31.4159	0.05	3.5×10^{9}	320000	0	1.3×10^{-9}	10937.5	142.942	104.58	0.68	45.971	0.01326	0.33	6.63	9.194
	10	62.8318	0.025	3.5×10^{9}	320000	0	1.3×10^{-9}	10937.5	285.885	104.59	1.37	45.974	0.01326	0.65	6.63	4.597
	50	314.159	0.005	3.5×10^{9}	320000	0	1.3×10^{-9}	10937.5	1429.423	104.80	6.82	46.068	0.01323	3.09	6.61	0.921
	100	628.318	0.0025	3.5×10^{9}	320000	0	1.3×10^{-9}	10937.5	2858.847	105.46	13.55	46.355	0.01315	5.83	6.57	0.464
	500	3141.59	0.0005	3.5×10^{9}	320000	0	1.3×10^{-9}	10937.5	14294.235	120.28	59.42	52.872	0.01153	19.80	5.76	0.106
	1000	6283.18	0.00025	3.5×10^{9}	320000	0	1.3×10^{-9}	10937.5	28588.469	144.13	99.18	63.354	0.00962	29.53	4.81	0.063
	2000	12566.36	0.000125	3.5×10^{9}	320000	0	1.3×10^{-9}	10937.5	57176.938	185.95	153.75	81.734	0.00746	42.54	3.73	0.041
	3000	18849.54	0.0000833	3.5×10^{9}	320000	0	1.3×10^{-9}	10937.5	85765.407	220.68	194.32	97.001	0.00628	52.33	3.14	0.032
	4000	25132.72	0.0000625	3.5×10^{9}	320000	0	1.3×10^{-9}	10937.5	114353.876	250.81	227.97	110.247	0.00553	60.53	2.76	0.028
Type II	1	6.28318	0.25	3.5×10^{9}	320000	7.409×10^{-14}	1.3×10^{-9}	10937.518	10.768	104.58	0.05	122.052	0.01326	0.08	6.63	122.052
	5	31.4159	0.05	3.5×10^{9}	320000	7.409×10^{-14}	1.3×10^{-9}	10937.939	53.853	104.58	0.26	122.063	0.01326	0.39	6.63	24.413
	10	62.8318	0.025	3.5×10^{9}	320000	7.409×10^{-14}	1.3×10^{-9}	10939.254	107.649	104.59	0.51	122.095	0.01326	0.78	6.63	12.210
	50	314.159	0.005	3.5×10^{9}	320000	7.409×10^{-14}	1.3×10^{-9}	10981.071	534.838	104.82	2.55	123.143	0.01323	3.83	6.61	2.463
	100	628.318	0.0025	3.5×10^{9}	320000	7.409×10^{-14}	1.3×10^{-9}	11108.404	1048.929	105.51	4.97	126.407	0.01314	7.47	6.57	1.264
	500	3141.59	0.0005	3.5×10^{9}	320000	7.409×10^{-14}	1.3×10^{-9}	13573.856	3236.138	117.32	13.79	227.785	0.01182	31.68	5.91	0.456
	1000	6283.18	0.00025	3.5×10^{9}	320000	7.409×10^{-14}	1.3×10^{-9}	15737.942	2946.281	125.99	11.69	537.39	0.01100	60.20	5.50	0.537
	2000	12566.36	0.000125	3.5×10^{9}	320000	7.409×10^{-14}	1.3×10^{-9}	16977.430	1853.509	130.49	7.10	1769.40	0.01062	120.00	5.31	0.885
	3000	18849.54	0.0000833	3.5×10^{9}	320000	7.409×10^{-14}	1.3×10^{-9}	17280.734	1297.724	131.55	4.93	3821.51	0.01054	181.14	5.27	1.274
	4000	25132.72	0.0000625	3.5×10^{9}	320000	7.409×10^{-14}	1.3×10^{-9}	17394.216	990.705	131.94	3.75	6694.27	0.01051	242.68	5.25	1.674

Values for the type I (conventional axon equivalent circuit) and type II (axon equivalent circuit with applied dielectrics) axon equivalent circuits computed in the framework of distributed-element circuit analysis. The vertical axis indicates the action potential rise velocity, expressed in the form of a frequency. The horizontal axis indicates the major quantities of interest computed via the equations described in section 2.9 and 2.10. The value of C_I in the type II circuit was chosen to yield a conduction velocity of $v = 120$ m/s utilizing the Equations (21) and (22) for an axon of diameter 20 μm at a rise frequency of 2,000 Hz.

constants given by Equations (16) and (17), respectively. The column labeled *Vr* indicates the raw velocity given by Equation (19), and the column labeled *L* indicates the maximum reachable distance given by Equation (20). The column labeled *v* indicates the conduction velocity *v* given by Equation (22) *x 1.23* for the conventional circuit and Equation (22) *x 1.48* for the proposed circuit, as mentioned at the end of section 2.11. The column labeled "Nodes/*L*" indicates the number of nodes of Ranvier within the maximum reachable distance *L*, and the column labeled "Wavelength" gives the wavelength computed as the ratio of the raw velocity to the frequency. At 2 kHz, the conduction velocity *v* in the conventional axon equivalent circuit is 42.5 m/s, and the raw velocity *Vr* is 81.7 m/s. In contrast, the conduction velocity *v* in the proposed axon equivalent circuit with applied dielectrics is 120.0 m/s, and the raw velocity *Vr* is 1,769.4 m/s. In this case, the propagation time is 0.068 s (120 m/1769 m/s) and the relay time 0.932 s, which indicates that the relay time is very long compared with the propagation time.

3.2 Plots of calculation results of two axon equivalent circuits

Table 2 gives the precise calculation results; however, it is difficult to understand the differences between the trends of the two axon equivalent circuits. Therefore, the trends of the two circuits are shown graphically in Figure 5a–e for the sake of clarity. In each of the plots in Figure 5a–e, the horizontal axis indicates the frequency, which is inversely proportional to the rise time. The thin red vertical line represents 2 kHz, which corresponds to a rise time of 125 µs. The black curves with triangles indicate the results of the conventional axon equivalent circuit, and the red curves with circles indicate the results of the axon equivalent circuit with applied dielectrics.

Raw velocity *Vr*: Figure 5a shows the raw velocity *Vr* of the two circuits. The raw velocity *Vr* of the conventional axon equivalent circuit increased slightly with increasing frequency from approximately 1 kHz, whereas the raw velocity *Vr* of the axon equivalent circuit with applied dielectrics increased exponentially with increasing frequency from approximately the same frequency. Therefore, the vertical axis is given in an exponential scale. The exponential trend strongly supports the effect of the axon fluid as a dielectric medium. However, the achieved velocity of 1,769 m/s at 2 kHz was very slow in comparison with the velocity of the conventional electric circuit; additionally, this velocity is approximately 1/170,000 of the speed of light (3×10^8 m/s).

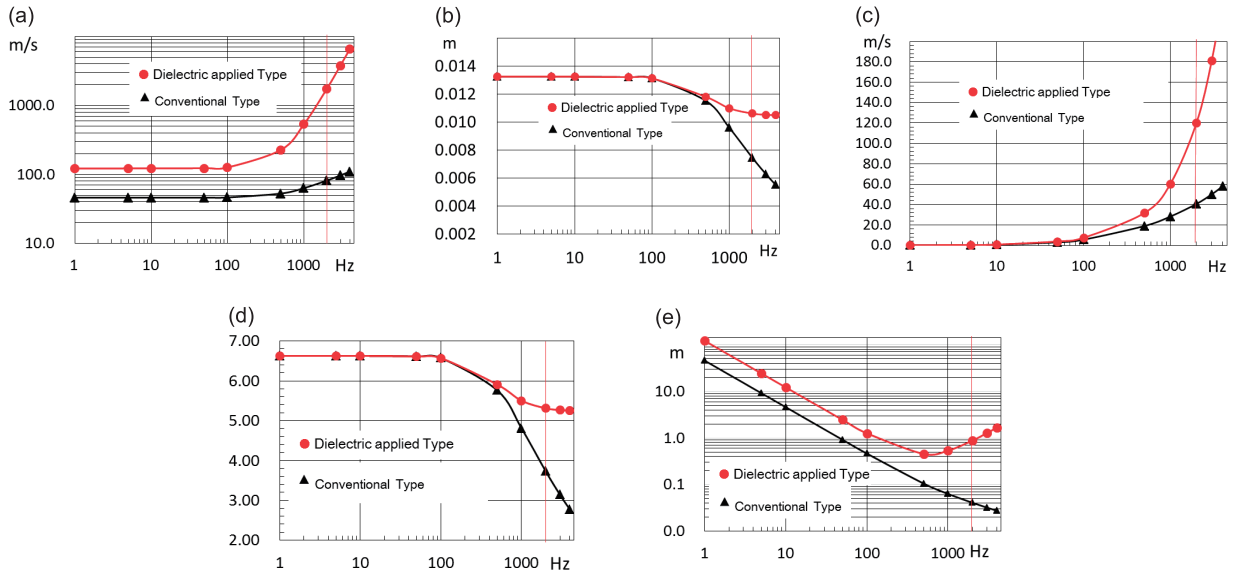

Figure 5 Computations for both types of axon equivalent circuits for axons of diameter 20 µm. The longitudinal capacitance C_l in the axon equivalent circuit was chosen with applied dielectrics to yield a conduction velocity of 120 m/s in 2 kHz. Black curves indicate results for the conventional axon equivalent circuit, and red curves are for the axon equivalent circuit with applied dielectrics. (a) Raw velocity *Vr*. Because the Raw velocity *Vr* increased exponentially beyond around 1 kHz for the axon equivalent circuit with applied dielectric, we used a logarithmic scale for the vertical axis as well as for the horizontal axis. Longitudinal capacitance C_l contributed largely to increase the raw velocity *Vr*. (b) Maximum reachable distance *L*. In the conventional axon equivalent circuit, the maximum reachable distance *L* rapidly decreased at frequencies beyond around 1 kHz. Longitudinal capacitance C_l prevented the maximum reachable distance *L* from becoming shorter. (c) Conduction velocity *v*. The slow values obtained for the conventional equivalent circuit at 2 kHz agreed with previously reported values [10–13]. In the axon equivalent circuit with applied dielectrics, the conduction velocity *v* 120 m/s is achieved. (d) number of nodes of Ranvier /*L*. The safety factor is relative to the number of nodes of Ranvier within the maximum reachable distance. In the axon equivalent circuit with applied dielectrics, number of nodes was five, even above 2 kHz, and for the conventional axon equivalent circuit, the number of nodes was three or below. (e) Wavelength. In the dielectric applied axon equivalent circuit with applied dielectrics, the raw velocity *Vr* was rapid, but still far below the speed of light, yielding a wavelength of 0.885 m at 2 kHz.

This reveals an important theme about the signal transmission property of axons, as will be discussed below in the subsection Wavelength. These results of raw velocity *Vr* support the understanding that the polarization of the axon fluid, a highly dielectric medium, acts as a carrier conveying the action potential.

Maximum reachable distance *L*: Figure 5b shows the maximum reachable distance *L* of the two circuits. In the conventional axon equivalent circuit, the leakage current produced by the displacement current through the axonal membrane capacitance C_2, which increases with increasing frequency, yielded a maximum reachable distance of less than 7.46 mm from approximately 1 kHz. In contrast, in the axon equivalent circuit with applied dielectrics, the longitudinal capacitance C_1 yielded a longitudinal displacement current that increased in proportion to the frequency. This compensated for the leakage current from the membrane capacitance C_2 and produced a maximum reachable distance of 10.62 mm, representing a lesser attenuation than in the conventional case.

Conduction velocity *v*: Figure 5c shows the conduction velocity *v* of the two circuits. The conduction velocity *v* of 120 m/s of the proposed axon equivalent circuit is higher than that of 42.54 m/s of the conventional circuit because the inclusion of the axonal longitudinal capacitance C_1 resulted in a higher raw velocity *Vr* faster and a larger maximum reachable distance *L*.

Number of nodes of Ranvier within the maximum reachable distance *L*: Figure 5d shows the number of nodes of Ranvier within the maximum reachable distance *L* for the two circuits. Even if defective nodes of Ranvier were present, the action potential could be propagated by the remaining nodes of Ranvier within the maximum reachable distance *L*. This number represents a safety factor [32].

Wavelength: Figure 5e shows the wavelength of an action potential in the two circuits. The data in this plot are valuable, as they indicate the wavelength of an action potential as it propagates through an axon. The significance of this is that if the wavelength is on the same order of magnitude as the circuit length through which signals pass, the signal is strongly affected by the circuit. Because the length of motor and sensory neurons is approximately 1 m and the wavelength of an action potential is 0.885 m, the length of the axons of these neurons cannot be ignored. However, the length of a uniform myelin sheath is 2 mm, approximately 1,000 times the 2 μm length of a node of Ranvier. Therefore, 99.9% of the axon length is composed of uniform regions of reasonable impedance, yielding a suitable transmission pathway as mentioned in the section 1.4. In other words, the myelin sheath may be considered as a structure to cope with the short wavelength of the action potential. In addition, the influence of the very low impedance of the node of Ranvier can be ignored because the ratio of the length of a node of Ranvier (2 μm) to that of the wavelength (0.885 m) is less than 1/440000. It is generally said that values below 1/100 can be considered negligible.

3.3 Applying the axon equivalent circuit with applied dielectrics to axons of different diameters

The conduction velocity *v* grows in proportion to the axon diameter [3,4]. Thus, from the value of the axon longitudinal capacitance C_1 determined by the procedure described above, Equation (1) was applied to scale this capacitance to axons of various diameters, and then the diameter-dependent values in Table 1 were applied as the circuit constants R_1, R_2, and C_2 in the axon equivalent circuit with applied dielectrics (see section 2.4). The results are shown in Figure 6a–e. The raw velocity *Vr* (Fig. 6a), the maximum reachable distance *L* (Fig. 6b), conduction velocity *v* (Fig. 6c), and the wavelength (Fig. 6e) were all found to be proportional to the axon diameter. However, because the spacing between the nodes of Ranvier and the maximum reachable distance *L* are also proportional to the diameter [4,17], the number of nodes of Ranvier contained within maximum reachable distance *L* (Fig. 6d) remained constant. This shows that the safety factor [32] is a constant independent of the conduction velocity *v* and the diameter of the axon. As shown in Figure 6c, the conduction velocities *v* of axons with diameters of 13 and 6 μm were 78 and 36 m/s, respectively. These are yield the same ratio of conduction velocity *v* to diameter as that for an axon diameter of 20 μm in diameter, i.e., the ratios of 120 m/s/20 μm, 78 m/s/13 μm and 36 m/s/6 μm are all the same value. These calculation results show that the preconditions and definitions considered in this study (section 2.12) are valid.

3.4 Comparison of relative permittivity of the longitudinal capacitance and the axon fluid

The aim of this study was to confirm the hypothesis that dielectric characteristics of axon fluid contributes to the conveyance of action potentials. To confirm this hypothesis, for an axon of 20 μm in diameter, the longitudinal capacitance necessary to achieve conduction velocity v of 120 m/s was calculated using the proposed axon equivalent circuit with applied dielectrics. The relative permittivity of an ionic fluid like axon fluid was compared with the relative permittivity calculated from the longitudinal capacitance using Equation (1). On the basis of the circuit constants given in Table 1, the value of longitudinal capacitance C1 was considered to be $C1 = 7.409 \times 10^{-14}$ F m. The relative permittivity ε_r corresponding to this C1 value calculated using Equation (1) was 1.33×10^7. This result would be ideally compared with the relative permittivity ε_r of actual axon fluid; however, this data could not be obtained. Therefore, we used the measurement data from [33] reporting the relative permittivity of an ionic fluid containing NaCl at 0.09 M; this is similar to axon fluid which is composed primarily of KCl at a concentration of 0.1 M. According to this, the relative permittivity of 0.09 M NaCl is approximately 3×10^7 at 0.2 kHz and 10^6 at 2 kHz. Therefore, the calculated value is in fair agreement

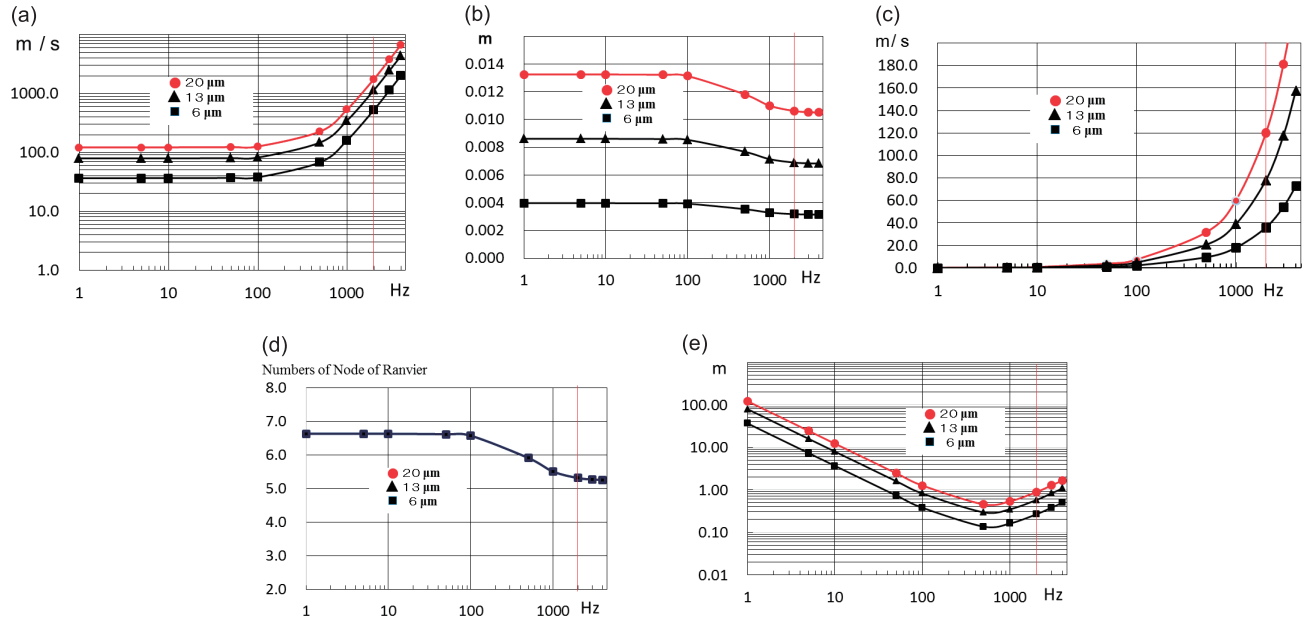

Figure 6 (a)–(e) Data comparison of axons of different diameters. (a)–(c) and (e) show the value which is proportional to the diameter. (a) shows the raw velocity *Vr*. (b) shows Maximum reachable distance *L*. (c) shows Conduction velocity *v*. (d) shows number of nodes of Ranvier /*L*. This figure shows that number of nodes of Ranvier being included in maximum reachable distance *L* is independent of the diameter. (e) shows Wavelength.

with the previously reported value. This result further confirms that the high-speed conduction of the action potential is achieved by a combination of the axonal characteristic morphology and the dielectric effect of the axon fluid.

4. Discussion

4.1 Equation for the conduction velocity of the action potential and axonal factors

As mentioned in sections 1.1 and 2.11, the conduction velocity v of the action potential depends on the relay interval x, the travel time t to reach the relay point x, and the relay time τ at the relay point x. The relay time τ is defined as the time from the start of an action potential until the voltage reaches the threshold of the voltage-gated Na channel.

$$v = x/(t+\tau) = x/\{(x/Vr) + A\sin(w/W/(1/e^{\alpha x}))/\omega\}. \qquad (21)$$

Equation (21) indicates that the conduction velocity v is determined by the angular velocity ω (rising speed of the action potential), the raw velocity Vr ($=\omega/\beta$), the attenuation constant α, the amplitude W of the action potential, and the attenuated amplitude w. The amplitude W is determined by capacitance C_n and voltage-gated Na channel density of node of Ranvier and the attenuated amplitude w is determined by the resting potential of the axon fluid and the threshold of the voltage-gated Na channel, and the attenuation constant α and phase constant β are determined from the wave equation of the action potential using the circuit constants R_1, R_2, C_1, and C_2. Therefore, it was demonstrated that conduction velocity v could be calculated quantitatively from the main electric factors representing the axonal morphology.

4.2 Characteristic axonal morphology and the axon fluid as a dielectric carrier

From the standpoint of electric circuit theory, the axon appears to comport rather naturally with the paradigm of distributed-element circuit analysis. Of course, distributed-element circuit modeling is typically reserved for signal frequencies of several hundred megahertz or more, but this conventional wisdom is based on the idea that signals pass through the electric circuits at nearly the speed of light. However, the degree of influence of the transmission line on the signal being transmitted depends on the ratio of the length of the transmission line to the wavelength of the signal. As stated in section 3.2, the wavelength of an action potential is 0.885 m at a frequency of 2 kHz, and the action potential is affected by an axonal transmission characteristic to approach the same level of length of the motor and sensory nerve. However, the properties of the myelin sheath make it a good transmission line, as mentioned in section 1.4. The morphology of the myelin sheath is a good complement to the extremely short wavelength of the action potential of the carrier of axon fluid. On the other hand, it becomes the domain where impedance is very low, where the membrane is very thin because the node of Ranvier does not have a sheath. However, the length of node of Ranvier region (2 μm) is very short compared with the wavelength (0.885 m), and it is less than 1/440000. Therefore, we thought that the quantity of energy loss of one wavelength of action potential

by node of Ranvier region is negligible. Rather, it is thought that this very short length is useful to ensure a low capacitance C_n of the node of Ranvier.

4.3 Steeply rising waveform of the action potential and voltage-gated Na channel density

A high raw velocity Vr and short relay time τ are necessary to achieve a high conduction velocity v. This means that the rise time from the start of the wave pattern of the action potential to its peak value is very important. As mentioned in section 2.7, it was considered in this study that the phenomenon of Na^+ ions flowing into the small capacitance C_n of the node of Ranvier via a large number of Na channels produces a steeply rising waveform characteristic of an action potential. Therefore, this rising phase was modeled as the first quarter period of a sine wave, which is similar to a charge curve.

In addition, according to a previous report [34,35] the channel of the voltage-gated Na channel is very narrow; it has been suggested that the time for a Na^+ ion to enter into the channel of same voltage-gated Na channel through which another Na^+ had just passed is required a time because of the thermal motion and the repulsion among Na^+ ions near the channel. Therefore, on the basis of the density of voltage-gated Na channels (12,000 sites/μm²) in the sciatic nerve of the rabbit reported by Ritchie (1977) [25], it is thought that the structure of the node of Ranvier enables the generation of a large amplitude and a steeply rising waveform if each of the Na channels operates with the same timing into the capacitance C_n of the node of Ranvier. From the standpoint of high density technology, we were surprised at the extremely high density of voltage-gated Na channel that is 1.2×10^{10}/mm², because this channel has complicate functions that recognizes Na ion and controls the path-way of Na ion depending on the voltage of action potential.

4.4 Collision between action potentials

The presence of multiple nodes of Ranvier within the maximum reachable distance L from a firing node senses the generated action potential and produces action potentials in response. Therefore, action potentials generate proximally in time and collide with one another. A collision of action potentials is a collision of waves of the form given in Equation (11). This equation demonstrates that action potentials propagate in both directions longitudinally along the axon with a raw velocity Vr ($= \omega/\beta$) and take on the temporal form of a sine wave of amplitude W that attenuates in space according to the attenuation constant α as mentioned in section 2.9. When action potentials collide, a wave equation that specifies when and where the action potentials were generated is added at the place of collision. In addition, the directions toward the axon terminal and the axon hillock were defined as positive and negative directions. Therefore, in the case of the collision of action potentials traveling in the same direction, their waveforms are added, and in the case of the collision of action potentials traveling in different directions, their waveforms are subtracted. On this basis, when an action potential traveling in the positive direction from the $(N-1)$th node of Ranvier meets an action potential traveling in the negative direction from the Nth node of Ranvier, it is eliminated if the amplitude of the positive traveling wave is smaller than that of the negative traveling wave. However, if the action potential from the $(N-1)$th node of Ranvier is not eliminated at the Nth node of Ranvier, the positive traveling action potential from the Nth node of Ranvier is added to it.

That is, the waveforms of (N − 1)th node of Ranvier are subtracted in the region before the Nth node of Ranvier and added in the region beyond this node. However, the phases of the added waves are different because each wave is generated independently.

4.5 Relative permittivity of ionic fluid similar to axon fluid

Using the axon equivalent circuit with applied dielectrics, the value of the capacitance C_l that yields a conduction velocity v of 120 m/s in an axon of 20 μm in diameter was calculated to be 7.41×10^{-14} Fm. The relative permittivity calculated using Equation (1) was very large (1.37×10^7) at this capacitance C_1. However, data on the frequency properties of the relative permittivity and electric current of axon fluid are not available. Thus, data on the frequency characteristics of relative permittivity and electric current were obtained for an ionic liquid composed of NaCl with a concentration of 0.09 M, which is similar to the KCl concentration of 0.1 M of axon fluid. Usually, it is less than 10^4 when the relative permittivity ε_r is high [36]; therefore, we were surprised at the value of the calculated relative permittivity ε_r of 1.37×10^7 of axon fluid, but we relieved to find the relative permittivity data of Gabriel [33]. From the previous report on the NaCl data, the permittivity is inversely proportional to the frequency, the growth rate of the electric current decreases with increasing frequency from 1 kHz, and the current is nearly flat near 10 kHz [33]. This trend suggests a balance point between the frequency of the axon fluid and the structure of the node of Ranvier. In addition, these extremely large values have been reported about the biological tissue, brain and heart [37–39]. In future study, we will examine the influence of the extremely high relative permittivity ε_r of the ion solution inside and outside neurons.

Conclusions

In this study, it was demonstrated that a high conduction velocity v of 120 m/s could be achieved when modeling an axon of 20 μm in diameter using a newly proposed axon equivalent circuit incorporating the dielectric behavior of the axon fluid as a longitudinal capacitance C_1. The raw velocity Vr for this conduction velocity v was 1769.4 m/s, and under the same conditions, the conventional axon equivalent circuit achieves a conduction velocity v of 42.5 m/s and a raw

velocity V of 81.7 m/s. These results show that propagation of the electric field produced by the polarization of the dielectric axon fluid acts as a carrier conveying action potentials. It was also demonstrated that the conduction velocity v calculated for axons of different diameters is proportional to the diameter. This is evidence of the validity of the definition of the longitudinal capacitance $C1$ and the proposed axon equivalent circuit with applied dielectrics. Furthermore, it was revealed that the long and uniform structure of the myelin sheath, which has a high impedance, is a good complement to the very short wavelength of the action potential and that the structure of the node of Ranvier enables the production of action potentials with a high amplitude and steep rise for the sake of fast raw velocity and short relay time. And we could indicate the equation (21) of conduction velocity v which includes all of main factors of axon. Finally, it was confirmed that the relative permittivity calculated from the longitudinal capacitance C_1 is very high (10^6–10^7) and nearly equal to the relative permittivity of an ionic fluid composed of NaCl with a concentration of 0.09 M, similar to the KCl concentration of 0.1 M in axon fluid. In this study, the circuit constants were used as listed in Table 1; these constants were derived by Hodgkin on the basis of data collected by Huxley, Stampfli, and Tasaki [20] in 1964 [19].

Acknowledgement

The authors would like to thank Dr. Naoki Yamamoto (Department of Psychiatry, Tokyo Metropolitan Tama Medical Center) and Dr. Toshihisa Shimizu (Department of Electrical and Electronic Engineer, Tokyo Metropolitan University) for their useful comments.

Conflicts of Interest

The authors declare no conflicts of interest. The authors declare no funding sources.

Informed Consent

In this study, the authors did not study humans in any experiments.

Author Contributions

TT: analyzed the conduction mechanisms for action potentials in myelinated neurons, developed and solved equations, conducted experiments involving ionic solutions, analyzed experimental data, drafted the article and revised important aspects of the intellectual content, approved the final version of the manuscript, agreed to be accountable for all aspects of the work, and ensured that questions related to the accuracy or integrity of any part of the work are appropriately investigated and resolved.

MK: approved the final version of the manuscript, agreed to be accountable for all aspects of the work, and ensured that questions related to the accuracy or integrity of any part of the work are appropriately investigated and resolved.

References

[1] Nicholls, J. G., Martin, A. R., Fuchs, P. A., Brown, D. A., Diamond, M. E. & Weisblat, D. A. *From Neuron to Brain 5th Edition* (Sinauer Associates, Inc., USA, 2012).
[2] Joshua, J. C. R. & Francisco, B. Seasonal Variation in Conduction Velocity of Action Potentials in Squid Giant Axons. *Biol. Bull.* **199**, 135–143 (2000).
[3] Boyd, I. A. & Kalu, K. U. Scaling factor relating conduction velocity and diameter for myelinated afferent nerve fibres in the cat hind limb. *J. Physiol.* **289**, 277–297 (1979).
[4] Hursh, J. B. Conduction Velocity and Diameter of Nerve Fibers. *American Journal of Physiology* **127**, 131–139 (1939).
[5] Stephen, G. & Waxman, M. Determinations of conduction velocity in myelinated nerve fibers. *Muscle & Nerve* **3**, 141–150 (1980).
[6] Ritchie, J. M. On the relation between fibre diameter and conduction velocity in myelinated nerve fibres. *Proc. R. Soc. London B Biol. Sci.* **217**, 29–35 (1982).
[7] Tasaki, I. The electro-saltatory transmission of the nerve impulse and the effect of narcosis upon the nerve fiber. *Am. J. Physiol.* **127**, 211–227 (1939).
[8] Huxley, A. F. & Stampfli, R. Evidence for salutatory conduction in peripheral myelinated nerve fibres. *J. Physiol.* **108**, 315–339 (1949).
[9] Tasaki, I. & Mizuguchi, K. Response of single Ranvier nodes to electrical stimuli. *J. Neurophysiol.* **11**, 295–303 (1948).
[10] Fitzhugh, R. Computation of impulse initiation and saltatory conduction in a myelinated nerve fiber. *Biophys. J.* **2**, 11–21 (1962).
[11] Goldman, L. & Albus, J. S. Computation of impulse conduction in myelinated fibers; Theoretical basis of the velocity-diameter relation. *Biophys. J.* **8**, 596–607 (1968).
[12] Moore, J. W., Joyner, R. W., Brill, M. H., Waxman, S. D. & Najar-Joa, M. Simulations of conduction in uniform myelinated fibers. Relative sensitivity to changes in nodal and internodal parameters. *Biophys. J.* **21**, 147–160 (1978).
[13] Stephanova, D. I. & Bostock, H. A distributed-parameter model of the myelinated human motor nerve fibre: temporal and spatial distributions of action potentials and ionic currents. *Biol. Cybern*. **73**, 275–280 (1995).
[14] Cestele, S., Qu, Y., Rogers, J. C., Rochat, H., Scheuer, T. & Catterall, W. A. Voltage Sensor-Trapping: Enhanced Activation of Sodium Channels by β-Scorpin Toxin Bound to the S3-S4 loop in Domain II. *Neuron* **21**, 919–931 (1998).
[15] Ramo, S. & Whinnery, J. R. *Fields and Waves in Modern Radio. 2nd Edition* (General Electric Company, 1953).
[16] Malmberg, C. G. & Maryott, A. A. Dielectric constant of water from 0° to 100°C. *Journal of Research of the National Bureau of Standard* **56**, 2641–2648 (1956).
[17] Vizoso, A. D. & Young, J. Z. Internode length and fibre diameter in developing and regenerating nerves. *J. Anat*. **82**, 110–134 (1948).
[18] Arancibia-Carcamo, I. L., Ford, M. C., Cossell, L., Ishida, K., Tohyama, K. & Attwell, D. Node of Ranvier length as a potential regulator of myelinated axon conduction speed. *Elife* e23329 (2017).
[19] Kenneth, S. C. *Membranes Ions and Impulses*. pp. 382–383 (University of California Press, 1972).
[20] Tasaki, I. New Measurement of the Capacity and the Resistance of the Myelin Sheath and the nodal membrane of the

Isolated Frog Nerve Fiber. *Am. J. Physiol*. **181**, 639–650 (1955).
[21] Hodgkin, A. L. & Huxley, A. F. A quantitative description of membrane current and its application to conduction and excitation in nerve. *J. Physiol.* **117**, 500–544 (1952).
[22] Peters, A. The node of Ranvier in the central nervous system. *Quart. J. Exp. Physiol.* **51**, 229–236 (1966).
[23] Zagoren, J. C. & Fedoroff, S. *Cellular neurobiology: A series. The node of Ranvier.* pp. 213–243 (Academic Press, Inc., 1984).
[24] Berthold, C. H., Nilsson, I. & Rydmark, M. Axon diameter and myelin sheath thickness in nerve fibers of the ventral spinal root of the seventh lumbar nerve of the adult and developing cat. *J. Anat.* **136**, 483–508 (1983).
[25] Ritchie, J. M. & Rogart, R. B. Density of sodium channels in mammalian myelinated nerve fibers and the nature of the axonal membrane under the myelin sheath. *Proc. Natl. Acad. Sci. USA* **74**, 211–215 (1977).
[26] Frankenhaeuser, B. & Huxley, A. F. The Action Potential in the Myelinated Nerve Fibre of *Xenopus laevis* as Computed on the Basis of Voltage Clamp Data. *J. Physiol.* **171**, 302–315 (1964).
[27] Huxley, A. F. & Stampfli, R. Direct determination of membrane resting potential and action potential in single myelinated nerve fibres. *J. Physiol.* **112**, 476–495 (1951).
[28] Tasaki, I. & Frank, K. Measurement of the action potential of myelinated nerve fiber. *Am. J. Physiol.* **182**, 572–578 (1955).
[29] Smit, J. E., Hanekom, T. & Hanekom, J. J. Modelled temperature-dependent excitability behavior of a signal Ranvier node for a human peripheral sensory nerve fibre. *Biol. Cybernetics* **100**, 49–58 (2009).
[30] Huxley, A. F. & Stampfli, R. Effect of potassium and sodium on resting and action potentials of single myelinated nerve fibres. *J. Physiol.* **112**, 496–508 (1951).
[31] Bear, M. F., Connors, B. W. & Paradiso, M. A. *Neuroscience: Exploring the Brain, Third edition. Chapter 3* (Nishimura Co., Ltd., 2007).
[32] Ushiyama, J. & Brooks, C. M. The Safety Factor for Conduction in Cardiac Muscle. *J. Physiol.* **13**, 231–239 (1963).
[33] Gabriel, S., Lau, R. W. & Gabriel, C. The dielectric properties of biological tissues: II. Measurement in the frequency range 10 Hz to 20 GHz. *Phys. Med. Biol.* **41**, 2251–2269 (1996).
[34] Catterall, W. A. Voltage-gated sodium channels at 60: structure, function and pathophysiology. *J. Physiol.* **590**, 2577–2589 (2012).
[35] Payandeh, J., Gamal E-Din, T. M., Scheuer, T., Zheng, N. & Catterrall, W. A. Crystal structure of a voltage-gated sodium channel in two potentially inactivated states. *Nature* **486**, 135–139 (2012).
[36] Lunkenheimer, P., Bobnar, V., Pronin, A. V., Ritus, A. I., Volkov, A. A. & Loidl, A. Origin of apparent colossal dielectric constants. *Phys. Rev. B* **66**, 052105-1-4 (2002).
[37] Martinsen, O. G., Grimnes, S. & Schwan, H. P. Interface phenomena and dielectric properties of biological tissue. *Encyclopedia of Surface and Colloid Science* **20**, 2643–2653 (2002).
[38] Gabriel, C., Gabriel, S. & Corthout, E. The dielectric properties of biological tissue: I. Literature survey. *Phys. Med. Biol.* **41**, 2231–2249 (1996).
[39] Gabriel, S., Lau, R. W. & Gabriel, C. The dielectric properties of biological tissues: III. Parametric models for the dielectric spectrum of tissues. *Phys. Med. Biol.* **41**, 2251–2269 (1996).